

Light-efficient beamsplitter for Fourier-domain full-field optical coherence tomography

EGIDIJUS AUKSORIUS^{1,2} 

¹Institut Langevin, ESPCI ParisTech, PSL Research University, CNRS UMR 7587, 1 rue Jussieu, 75005 Paris, France

²Institute of Physical Chemistry, Polish Academy of Sciences, Kasprzaka 44/52, 01-224 Warsaw, Poland (egidijus.auksorius@gmail.com)

Received 21 November 2019; revised 20 January 2020; accepted 29 January 2020; posted 29 January 2020 (Doc. ID 383823); published 27 February 2020

Any full-field optical coherence tomography (FF-OCT) system wastes almost 75% of light, including 50% of the OCT signal, because it uses a 50/50 beamsplitter (BS) in the standard implementation. Here, a design of a light-efficient BS is presented that loses almost no light when implemented in Fourier-domain FF-OCT. It is based on pupil engineering and a small highly asymmetric BS. The presented signal-to-noise ratio (SNR) analysis demonstrates almost four times improvement over the conventional design. In addition, it is shown that the light-efficient BS can be used to suppress specular reflections from a sample and, thus, further improve the SNR. © 2020 Optical Society of America

<https://doi.org/10.1364/OL.383823>

Full-field optical coherence tomography (FF-OCT) can acquire *en face* OCT images by using a camera [1]. Conventional FF-OCT, operating in the time-domain, uses a spatially incoherent light source that together with high-NA objectives enables high-resolution and crosstalk-free imaging. However, FF-OCT is relatively slow for the volumetric (3D) imaging, and, thus, Fourier-domain FF-OCT (FD-FF-OCT) has recently been developed that employs a swept laser source in conjunction with a very fast camera [2–4]. Also known as full-field swept-source optical coherence tomography (FF-SS-OCT), it can achieve voxel rates of up to 10 GHz [4], making it one of the fastest volumetric OCT imaging techniques. However, the absence of the confocal pinhole in the wide-field detection makes it more sensitive to incoherent light, such as specular reflections and multiply scattered light. Unlike scanning OCT, where power of the swept laser sources is rarely an issue, it may be too weak for FF-OCT. Furthermore, a typical wide-field interferometer in FF-OCT wastes almost 75% of light budget due to the use of a 50/50 beamsplitter (BS). Namely, the BS rejects 50% of light going from the light source to the sample and another 50% when backscattered light goes from the sample to the camera. The loss of the OCT signal is particularly problematic when imaging photosensitive samples, such as the eye, since losses cannot be compensated by increasing the power due to the eye safety considerations. Light in the reference arm is practically all lost since it is strongly attenuated for the optimal SNR when imaging biomedical samples [1].

Here, a concept of a light-efficient BS is described that loses only a small portion of light ($< 1\%$) when imaging typical biomedical samples. Moreover, the BS can reject specular reflections coming from a sample, if properly aligned, thanks to the dark-field mode. The principle exploits the fact that the OCT signal is derived from the backscattered light that is normally scattered across a wide range of angles, whereas the reference beam is sent back at one angle in a spatially coherent illumination case, as shown in Fig. 1. Therefore, a BS can be designed such that it either transmits or reflects the incoming photons depending on their propagation angle. Since the spatially coherent beam is focused to a diffraction limited spot in the pupil plane of an objective lens in the Linnik interferometer, as shown in Fig. 2, the BS can be made less than 1 mm in diameter. It can be mounted on a glass substrate and placed in the middle of the pupil plane of the objective lens. Such a small BS with a 50/50 beam splitting ratio would already be nearly twice more efficient in detecting backscattered light from the sample compared to, for example, regular-sized 50/50 BS. The small BS lets the backscattered light from the sample travel freely toward the camera and blocks only a small part of it, as shown in Figs. 1(b) and 2(a), whereas the conventional 50/50 BS rejects half of the photons. Furthermore, the splitting ratio of the small BS can be made highly asymmetric, such as 99/1, which would send most of the light to the sample and only a small part of it (1%) to the reference mirror. Combining almost twice more efficient illumination and detection results in the overall four times throughput improvement in the limited light-budget situations. Below it will be shown that the throughput improvement also translates to the four times increase in the SNR. Light in the reference arm is reflected by the reference mirror and the BS to the camera almost without losses.

Light traveling from the sample through the 99/1 BS would be attenuated by 20 dB meaning that it can efficiently reject specular reflections. Since specular reflections coming from a sample or other element in the system in general compromise the performance of FF-OCT, its rejection can improve the SNR. Strong specular reflections could appear from a cover glass that is routinely used for mounting cell preparations [5] and tissue slices [6]. The use of immersion medium or tilting a sample [7] to reduce specular reflections is not always possible or practical. It has been previously demonstrated that specular reflections can be rejected in a high-resolution FF-OCT system

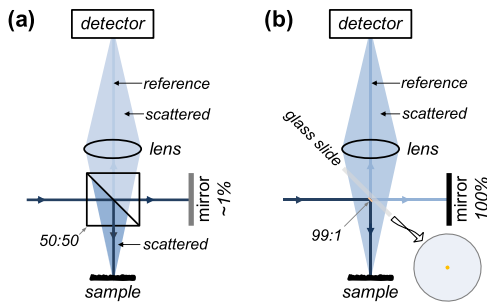


Fig. 1. (a) Standard configuration with a 50/50 beamsplitter (BS) and a weak reflector. (b) A light-efficient BS configuration with 99/1 BS mounted in the middle of a glass substrate, which lets the backscattered signal through without significant losses. The BS will also reject specular reflections from a sample back to the laser source if the reflections are made to travel back the same path.

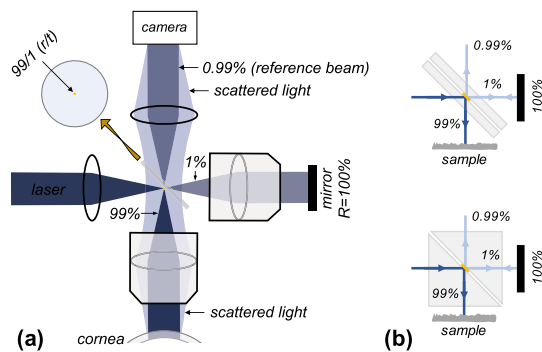


Fig. 2. (a) FF-OCT with light-efficient BS in Linnik-type interferometer. Beamsplitting is performed by a small 99/1 (r/t) plate BS, less than 1 mm in diameter, mounted on a glass plate in the middle of the pupil. (b) Achromatic designs of a light-efficient BS. A 99/1 BS (in yellow) is sandwiched between the two antireflection-coated glass slides (top) and prisms (bottom) that freely transmit the backscattered light propagating off-axis from cornea. The former design avoids ghost reflections from the BS's surface.

by placing a block in the pupil plane of the detection path [6]. Since dark-field detection is realized in the pupil plane, the orientation of the reflecting surface in the sample plane becomes critical. Therefore, to ensure that specular reflections do not miss the small 99/1 BS, the orientation of a sample needs to be controlled. For example, a tip and tilt stage was used previously to adjust a window that produced specular reflections at its interface with skin when imaging it *in vivo* with dark-field FF-OCT [6]. In another implementation, an additional mirror was placed between the BS and sample [8], to enable directing specularly reflected light back to the light source. In a similar way, the direction of specular reflections coming from glass slides with cells [5] or tissue [6] mounted behind a coverslip, could be controlled. The throughput problem in confocal scanning OCT is solved by using a fiber optical circulator [9] that improves the SNR by a factor of 4. However, it would require a large aperture Faraday rotator in its wide-field implementation, which is practically not feasible. Polarization crosstalk of a polarizing BS was also demonstrated to improve the SNR in scanning OCT [10]. To demonstrate the SNR advantage of the light-efficient BS a theoretical noise analysis is performed below. The total number

of photons, N_{det} detected by the camera can be expressed as

$$N_{\text{det}} = N_R + N_O + N_{\text{inc}} + 2\sqrt{N_R N_O} \cos(\phi), \quad (1)$$

where N_R is the number of photons returned from the reference arm, N_O and N_{inc} are the coherent and incoherent photon numbers, respectively, coming from the sample arm, and ϕ is the phase between the sample and the reference arms. It can be shown that the OCT signal is proportional to $N_R N_O$ and noise to $N_R + N_{\text{inc}} + nee^2$, where N_O is disregarded (since $N_{\text{inc}} \gg N_O$ in biological samples) and nee is the noise equivalent electrons that account for all the electrical noises in the camera. One can, therefore, define the SNR in FF-OCT as

$$\text{SNR} = \frac{\text{signal}}{\text{noise}} \propto \frac{N_R N_O}{N_R + N_{\text{inc}} + nee^2}. \quad (2)$$

If N is the total number of photons entering the standard interferometer, shown in Fig. 1(a), and r, t are the reflectance and transmittance values of the BS, the numbers of photons N_R, N_O , and N_{inc} reaching the camera can then be expressed as

$$N_R = Nr t R_R, \quad N_O = Nr t R_O, \quad N_{\text{inc}} = Nr t R_{\text{inc}}, \quad (3)$$

where R_R, R_O , and R_{inc} are the corresponding reflectivity values. It is assumed here that the BS reflects toward the sample. For the light-efficient BS, shown in Fig. 1(b), the numbers of detected photons will be accordingly:

$$N_R = Nr t R_R, \quad N_O = Nr T R_O, \quad N_{\text{inc}} = Nr T R_{\text{inc}}, \quad (4)$$

where T is the transmission of the light-efficient BS from the sample to the camera, which is close to 100% when the asymmetric BS is small. One can see that t in Eq. (3) is simply replaced by T in Eq. (4) for the sample arm.

The signal loss due to the asymmetric BS physically blocking the backscattered light in the pupil plane can be defined as the ratio between the areas of the asymmetric BS and that of the pupil: $\frac{\pi(d/2)^2}{\pi(D/2)^2}$, where d and D are their diameters, respectively. Here, it was assumed that the backscattered light from the sample is distributed homogeneously in the pupil plane of the objective lens, which should be true for isotropically scattering samples. Subtracting the losses from the unity one can define the transmission, T , from the sample to the detector as

$$T = 1 - \frac{d^2}{D^2}. \quad (5)$$

In principle, d can be as small as the size of the focused laser spot. Since the divergence of the laser beam reflected off from the BS should be within the objective's acceptance angle, defined by the numerical aperture (NA), the relation $d \geq \lambda/NA$ should be satisfied. Since typically $D \gg d$, the value of T is close to 100%. For the $\times 10$ objective (NA = 0.25), typically used for high-resolution FF-OCT, D is ~ 1 cm and d is $\geq 4 \mu\text{m}$ (at 850 nm), resulting in $T \approx 100\%$. Even when a more practical BS size of 1 mm is used it still results in 99% of photons transmitted from the sample to the detector. To see how efficiently the photons are routed from the laser source to the camera, we can define the light efficiency, E , as $\frac{N_{\text{det}}}{N}$, where N_{det} is the number of detected photons. We can subsequently write, using Eq. (4), that the photon numbers coming from the reference and sample arms

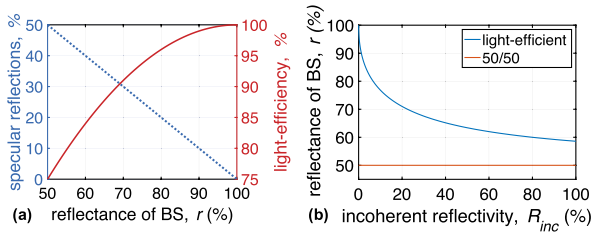


Fig. 3. (a) Light efficiency (red curve) and transmission of specular reflections to the camera (blue-dotted curve), as a function of the BS reflectance, r . (b) Optimal BS reflectance, r as a function of incoherent reflectivity, R_{inc} for the light-efficient (blue curve) and regular 50/50 (red curve) BSs.

are as follows: $N_{det} = N_R + N_O = Nr(tR_R + TR_O)$, which does not include the incoherent light contribution. Further, by using a (slightly tilted) mirror as a sample and a (normally oriented) mirror as the reference reflector, we can rewrite the last equation as $N_{det} = Nr(t + T)$. Finally, replacing t with $1 - r$, and expressing for $\frac{N_{det}}{N}$, we can write the light efficiency, E , as

$$E = r(1 - r + T). \quad (6)$$

For example, when $r = 99\%$ and $T = 99\%$ [for the 1 mm BS diameter, as calculated using Eq. (5)], the light-efficient BS uses 99% of the laser light, meaning that in total only 1% of light is lost. Figure 3(a) shows light efficiency as a function of the BS reflectance, r . The light efficiency in the conventional configuration, shown in Fig. 1(a), is only $\sim 25\%$ —almost four times less. The SNR expression in Eq. (2) can be rewritten for the regular FF-OCT using Eq. (3), which can be further simplified assuming that nee is negligible:

$$\text{SNR}_{\text{regular}} \propto N \frac{rtR_R R_O}{R_R + R_{inc}}. \quad (7)$$

Similarly, using equations in Eq. (4) we can get the SNR expression for the light-efficient interferometer as

$$\text{SNR}_{\text{efficient}} \propto N \frac{rtR_R R_O T}{tR_R + TR_{inc}}. \quad (8)$$

When the light budget is limited, one can increase the reference mirror reflectance to the highest value of 100% ($R_R = 1$), in order to get the largest possible number of photons from the reference on the camera. Here it is assumed that the relative intensity noise (RIN) can be ignored. Further, replacing t with $1 - r$, we can simplify Eq. (7) to

$$\text{SNR}_{\text{regular}} \propto \text{NR}_O \frac{r(1 - r)}{1 + R_{inc}}, \quad (9)$$

and Eq. (8) to

$$\text{SNR}_{\text{efficient}} \propto \text{NR}_O \frac{r(1 - r)T}{1 - r + TR_{inc}} \approx \text{NR}_O \frac{r(1 - r)}{1 - r + R_{inc}}. \quad (10)$$

The transmission, T , is close to 100% and, thus, could be ignored. To find the optimal reflectance, r , of the light-efficient BS, the derivative of Eq. (10) is first found and equated to zero:

$$\frac{r^2 - 2rR_{inc} - 2r + R_{inc} + 1}{(1 - r + R_{inc})^2} = 0. \quad (11)$$

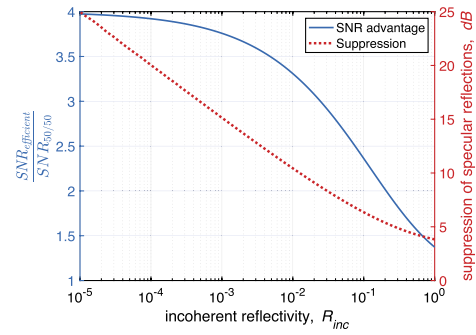


Fig. 4. SNR advantage (blue curve) and suppression of specular reflections coming from the sample (dotted red curve), as a function of the incoherent reflectivity R_{inc} .

Solving Eq. (11) for r , the optimal BS reflectance is found as

$$r = R_{inc} + 1 - \sqrt{R_{inc}(R_{inc} + 1)}. \quad (12)$$

Likewise, we can show that the optimal BS's reflectance in the regular system will always be $r = 0.5$ —independent of R_{inc} . Namely, differentiating Eq. (9) and equating it to zero results in $2r - 1 = 0$, which is then solved as $r = 0.5$. Figure 3(b) shows the optimal reflectivity, r , as a function of R_{inc} for the regular and light-efficient implementations. When incoherent light becomes small, say $R_{inc} = 1\%$, the optimal beamsplitting ratio is then 91/9. For the systems, drawn in Figs. 1(b) and 2(a), the light-efficient BS with the 99/1 splitting ratio will be optimal for $R_{inc} = 0.01\%$. When R_{inc} becomes small, Eq. (9) can be further approximated to

$$\text{SNR}_{\text{regular}} \propto 0.25 \text{NR}_O, \quad (13)$$

and Eq. (10) to

$$\text{SNR}_{\text{efficient}} \propto r \text{NR}_O. \quad (14)$$

This is known as the shot-noise-limited detection where the SNR is independent of the reference reflectance. Namely, this happens when the reference arm shot-noise dominates over other sources, such as sample arm shot-noise and camera noise. Dividing Eq. (13) by Eq. (14), the SNR advantage of the light-efficient implementation over the standard one can then be expressed in this operating regime as

$$\frac{\text{SNR}_{\text{efficient}}}{\text{SNR}_{\text{regular}}} = 4r. \quad (15)$$

It approaches the value of 4 with $r \rightarrow 1$, which, in turn, happens with $R_{inc} \rightarrow 0$, as follows from Eq. (12). Figure 4 shows the SNR advantage of the light-efficient configuration as a function of R_{inc} . One can see that the SNR advantage will become small when R_{inc} is close to 100% but will not be completely lost. A similar approach [8,11] requires a regular-size 90/10 (or similar) BS and engineered mirror but achieves lower SNR improvement.

As discussed above, the light-efficient BS could also function in the dark-field mode since the BS is able to attenuate reflections going to the camera by a factor of $1/(1 - r)$. Figure 3(a) shows the transmission of specular reflections as a function of the light-efficient BS reflection (blue curve). For the 99/1 beamsplitting, specular reflections will be attenuated to 1%

or $10 \log\left(\frac{1}{1-r}\right) = 20$ dB. Since the transmission is a function of the BS reflectance, r [blue curve in Fig. 3(a)], which in turn is a function of the incoherent reflectivity, R_{inc} [blue curve in Fig. 3(b)], one can plot the suppression [inverse of transmission plotted in Fig. 3(a)] of specular reflections as a function of R_{inc} ; this is shown in Fig. 4 (red curve). Blocking the specular reflections should also reduce the autocorrelation noise in FD-FF-OCT, which has been done before computationally by filtering out the DC term in the Fourier space [2]. However, unlike the computational approach, the light-efficient BS will be unable to increase the imaging range because it cannot remove the conjugate term. Since the pupil plane in objectives is sometimes inside the objective body and, therefore, not accessible, relay lenses can be used to reimage the pupil plane to an accessible location, like in Ref. [6]. If using the light-efficient BS with the conventional (time-domain) FF-OCT, losses will be incurred associated with the high *étendue* of the spatially incoherent source, such as LED. Specifically, the size of the asymmetric BS will have to be considerable in order not to lose too much of the illumination light but at the expense of the reduced transmission T , as follows from Eq. (5). Conventional FF-OCT, unlike FD-FF-OCT, requires dispersion matching between the two arms. Figure 2(b) shows two possible achromatic designs that have an equal amount of dispersion introduced in both arms by the symmetric design. If a multilayer antireflection coating with average reflectance of 0.2% is applied to all the BS surfaces, the losses in the number of detected photons will be only 1.2 % (assuming photons encounter six surfaces in total), resulting in SNR reduction by only 0.05 dB, as follows from Eq. (14). Reflections will also be insignificant but should be prevented from reaching the camera, which can be done by rotating the BS, shown at the bottom of Fig. 2(b), by a small degree [12]. A multilayer coating can also be used to make the 99/1 BS by physical vapor deposition. The ability of the light-efficient design in the FF-OCT system to deliver more light to the sample and to collect more signal from it should be particularly useful for the imaging cornea [13] and retina [4]. An inherent dark-field detection feature of the BS should also be useful for imaging the cornea at the apex where strong specular reflections occurs from the air-tear film. Since the radius, R , of the central corneal curvature is 7.8 mm, it will act as a convex reflector with the focal length of $f_c = R/2 = 3.9$ mm, making cornea imaging more complex than that of flat samples. The cornea will form a virtual focus of specular reflections at the distance of f_c beneath its surface. It can be shown that the reflections will be focused by the objective lens at the distance of f_{obj}^2/f_c behind the 99/1 mirror, magnified by $M = f_{\text{obj}}/f_c$, where f_{obj} is the focal length of the objective. The beam size on the 99/1 mirror will then be $M \times \text{FOV}$, where FOV is the imaging field of view. Note, that magnification, M of specular beams is different to the image magnification, which is usually chosen to be $\times 10$ for high-resolution cornea imaging [13]. If $\text{FOV} = 0.5$ mm, then the beam size on the 1 mm 99/1 mirror will also be 0.5 mm, when $f_{\text{obj}} = f_c = 3.9$ mm ($M = 1$). If a Gaussian beam shape is assumed, the resulting suppression of specular reflections by the mirror is then 98%. For the $\times 10$ image magnification a tube lens of 39 mm would need to be used. The lowest possible magnification, M , of specular reflections is also important to make the dark-field detection less sensitive to the eye motion since lateral eye displacement by dx

will result in the displacement of the beam by Mdx on the 99/1 mirror. When $M = 1$, aligning the eye for dark-field operation can be carried out with a chin rest equipped with the x and y translation stage, which is routinely used for cornea FF-OCT imaging. To avoid the laser being focused to a spot on the retina, which can cause damage, the spatial coherence of the laser can be destroyed by a fast-deformable membrane [12,14], resulting in a broader laser spot on the retina. The broadening will also slightly offset the suppression of specular reflections by the 99/1 mirror.

In conclusion, the light-efficient BS was presented that can improve the SNR when the light budget is limited. It was shown that the losses sustained in the regular FD-FF-OCT interferometer, amounting to 75 % of the total light budget, can be decreased to the negligible values, translating to a $\times 4$ SNR increase. The BS design in FF-OCT was based on the pupil engineering that decouples the reflectance of the BS from its transmission and, thus, enables use of highly asymmetric beamsplitting ratios. The design also allows rejection of specular reflections, which can saturate the camera and introduce the autocorrelation noise in FD-FF-OCT. The diameter of the asymmetric BS can be made relatively small, since lasers have low *étendue*, even when its spatial coherence is destroyed for the crosstalk reduction [14], naturally making it optimal for the spatially semicoherent crosstalk-free FD-FF-OCT. In crosstalk-free retina imaging with FD-FF-OCT [12] it is also expected to improve the SNR by up to four times.

Funding. Horizon 2020 Framework Programme (666295).

Acknowledgment. The author thanks Claude Boccara and Maciej Wojtkowski for useful discussions.

Disclosures. The author declares no conflicts of interest.

REFERENCES

1. A. Dubois, L. Vabre, A. C. Boccara, and E. Beaufrepaire, *Appl. Opt.* **41**, 805 (2002).
2. D. Hillmann, H. Spahr, H. Sudkamp, C. Hain, L. Hinkel, G. Franke, and G. Huettmann, *Opt. Express* **25**, 27770 (2017).
3. H. Spahr, D. Hillmann, C. Hain, C. Pfäffle, H. Sudkamp, G. Franke, and G. Huettmann, *Opt. Lett.* **40**, 4771 (2015).
4. D. Hillmann, H. Spahr, C. Hain, H. Sudkamp, G. Franke, C. Pfäffle, C. Winter, and G. Huettmann, *Sci. Rep.* **6**, 35209 (2016).
5. M. Villiger, C. Pache, and T. Lasser, *Opt. Lett.* **35**, 3489 (2010).
6. E. Auksorius and A. C. Boccara, *Opt. Lett.* **40**, 3272 (2015).
7. L. Vabre, V. Lorient, A. Dubois, J. Moreau, and A. C. Boccara, *Opt. Lett.* **27**, 1899 (2002).
8. E. Auksorius and A. C. Boccara, *Opt. Lett.* **45**, 455 (2020).
9. B. E. Bouma and G. J. Tearney, *Opt. Lett.* **24**, 531 (1999).
10. N. Lippok, P. Nielsen, and F. Vanholsbeeck, *Opt. Express* **19**, 7161 (2011).
11. E. Auksorius and A. C. Boccara, "Full-field interferential imaging systems and methods," U.S. patent application 16/320,982 (06 June 2019).
12. E. Auksorius, D. Borycki, and M. Wojtkowski, *Biomed. Opt. Express* **10**, 6390 (2019).
13. V. Mazlin, P. Xiao, E. Dalimier, K. Grieve, K. Irsch, J.-A. Sahel, M. Fink, and A. C. Boccara, *Biomed. Opt. Express* **9**, 557 (2018).
14. P. Stremplewski, E. Auksorius, P. Wnuk, Ł. Kozoń, P. Garstecki, and M. Wojtkowski, *Optica* **6**, 608 (2019).